Lattice Evidence that Scalar Glueballs Are Small

Ryan Abbott,[1] Daniel C. Hackett,[2] Dimitra A. Pefkou,[3,4,*] Fernando Romero-López,[5] and Phiala E. Shanahan[1]
[1]*Center for Theoretical Physics—A Leinweber Institute, Massachusetts Institute of Technology, Cambridge, Massachusetts 02139, USA*
[2]*Fermi National Accelerator Laboratory, Batavia, Illinois 60510, USA*
[3]*Department of Physics, University of California, Berkeley, California 94720, USA*
[4]*Nuclear Science Division, Lawrence Berkeley National Laboratory, Berkeley, California 94720, USA*
[5]*Albert Einstein Center, Institute for Theoretical Physics, University of Bern, 3012 Bern, Switzerland*

(Received 12 September 2025; revised 21 November 2025; accepted 3 December 2025; published 26 January 2026)

This Letter reports the first calculation of the gravitational form factors (GFFs) of the scalar glueball, performed via lattice field theory in Yang-Mills theory at a single lattice spacing. The glueball GFFs are compared with those of other hadrons as determined in previous lattice calculations, providing strong indications that glueballs have a different gluonic structure than typical hadronic states. A mass radius of 0.263(31) fm is predicted, supporting previous suggestions that the scalar glueball is significantly smaller than other hadrons.

DOI: 10.1103/67xg-qxhz

Introduction—Since the inception of quantum chromodynamics (QCD) [1], glueballs have been postulated as hadronic states with purely gluonic degrees of freedom. Decades of experiments in hadron spectroscopy have collected experimental glueball candidates with a variety of allowed quantum numbers, e.g., $J^{PC} = 0^{++}, 0^{-+}, 1^{++}, 1^{+-}, 1^{--}, 2^{++}$, etc. [2–7]. Lattice calculations of hadronic resonances provide valuable guidance toward the identification of putative glueball states [8–14]—see Refs. [15,16] for a review. However, identifying observed hadrons as glueballs or glueball-like states based on spectroscopy remains challenging due to the mixing of hadrons with the same quantum numbers [17,18].

Beyond the spectrum, information about the internal structure of hadrons may provide an additional pathway for classification of observed states as glueball-like or nonglueball objects. For example, features such as the momentum fraction carried by gluons may be qualitatively different for glueball and nonglueball states, and could serve as evidence of a hadron having predominantly gluonic degrees of freedom. The size of glueballs, which can be defined in various ways, can serve as another way to distinguish them from typical hadrons; model studies [19–21] have speculated that the scalar glueball might be more compact than the Λ_{QCD} scale that is thought to define the size of more typical hadrons. This was supported by early lattice studies which, however, relied on smearing arguments [22] or a model-dependent Bethe-Salpeter approach to define the radius [23,24], or were performed in $SU(2)$ Yang-Mills theory [25,26]. The typical scales found, around 0.2 fm, are also significantly smaller than the radius of the σ meson, which is the lightest resonance with the same quantum numbers, as predicted from a dispersive analysis [27].

The *gravitational form factors* (GFFs) of hadrons encode the gluon momentum fraction and distribution of quantities like the energy inside hadrons [28], offering a robust way to define their size through, e.g., their mass radius, defined from the root mean square of the energy density. The GFFs are defined from the matrix elements of the *energy-momentum tensor* (EMT) $T^{\mu\nu}$ of QCD [28–31]. Lattice QCD provides a tool to determine these matrix elements, and thus the glueball GFFs. While previous pioneering work [25,26,32] has investigated glueball matrix elements using lattice field theory, the GFFs of glueballs have not been previously constrained.

This Letter presents a first step toward quantitative studies of glueball structure through a calculation of the GFFs of the lowest-lying scalar glueball state (see Ref. [33] for preliminary results of this Letter) denoted as $G[0^{++}]$, in $SU(3)$ Yang-Mills theory. In a pure gauge theory, the EMT is purely gluonic, defined as $T^{\mu\nu} = 2\mathrm{Tr}[-F^{\mu}_{\alpha}F^{\alpha\nu} + \frac{1}{4}g^{\mu\nu}F^{\alpha\beta}F_{\alpha\beta}]$, where $F^{\mu\nu}$ is the gluon field strength tensor. The EMT matrix element for the scalar glueball can be decomposed in terms of two GFFs, $A(t)$ and $D(t)$ [34–36]:

$$\langle G[0^{++}](p')|T^{\mu\nu}|G[0^{++}](p)\rangle = 2P^{\mu}P^{\nu}A(t) + \frac{\Delta^{\mu}\Delta^{\nu} - g^{\mu\nu}\Delta^2}{2}D(t), \quad (1)$$

[*]Contact author: dpefkou@berkeley.edu

where the four-momenta of the incoming and outgoing states are denoted p and p', $P = (p + p')/2$, $\Delta = p' - p$, and $t = \Delta^2$. Note that $A(0) = 1$ follows from the momentum sum rule [35], while the D-term, $D(0)$, is an unconstrained and previously unknown quantity.

Methodology—Calculations are performed using a single pure-gauge ensemble defined by the $SU(3)$ Wilson gauge action with $\beta = 5.95$. This results in $a = 0.098$ fm, using the Sommer parameter to set the scale [37,38]. The lattice geometry is $L^3 \times T = 24^3 \times 48$. Calculations are performed using $\mathcal{O}(10^7)$ configurations generated using $\mathcal{O}(10^5)$ independent streams of heatbath with overrelaxation [39–43], which were saved every 25 heatbath hits. Two-point correlation functions are constructed on each configuration using two interpolating operators,

$$\chi_1(x) = \frac{1}{4}\sum_{\mu\neq\nu}\mathrm{ReTr}U^2_{\mu\nu}(x),$$
$$\chi_2(x) = \frac{1}{4}\sum_{\mu\neq\nu}\mathrm{ReTr}U^7_{\mu\nu}(x), \tag{2}$$

where $\mu,\nu \in \{x, y, z\}$. Here, $U^n_{\mu\nu}$ is an $n \times n$ Wilson loop which extends in the μ and ν directions constructed from links stout smeared [44] by 3 steps in the spatial directions only. It is convenient to define vacuum-subtracted operators of definite three-momentum $\mathbf{p}$ as

$$\chi_i(\mathbf{p}, t) = \sum_{\mathbf{x}} e^{-i\mathbf{p}\cdot\mathbf{x}}\Big[\chi_i(\mathbf{x}, t) - \langle\chi_i(\mathbf{x}, t)\rangle\Big]. \tag{3}$$

The positive-parity 0^{++} glueball is the lowest-energy state excited by these operators; the summations over μ, ν in Eq. (2) project to the A_1^+ (rest frame) or A_1 (moving frames) irreducible representations (irreps) of the finite-volume symmetry group, while taking the real part projects to positive charge conjugation quantum numbers. These irreps have maximal overlap with the scalar glueball; however, depending on the momentum frame, the spectrum may also include heavier glueballs with other quantum numbers, e.g., tensor or pseudoscalar glueballs, or multiglueball or higher-lying ditorelon states [45]. Note that in QCD, as opposed to Yang-Mills theory as studied here, the situation is far more complicated because of mixing between glueball and mesonic operators [17,18].

The spectrum of glueball states is constrained via the generalized eigenvalue problem (GEVP) method [46–52]. The GEVP is applied to the 2×2 matrix of momentum-projected two-point functions averaged over all time slices:

$$C^{2\mathrm{pt}}_{ij}(\mathbf{p}, t) = \frac{1}{T}\sum_{t_0}\langle\chi_i(\mathbf{p}, t + t_0)\chi_j(\mathbf{p}, t_0)^\dagger\rangle \tag{4}$$

for all $|\mathbf{p}|^2 \leq 6(2\pi/L)^2$ on 200 bootstrap ensembles after binning the $\mathcal{O}(10^7)$ configurations into groups of 1000 consecutive configurations. Averaging over equivalent momenta yields two-point functions for the seven distinct $|\mathbf{p}|^2$; analyzing them in a "fixed pivot" [46–48] mode with $t_0 = 1$ and diagonalization time $t_d = 3$ gives seven sets of weights $w_{ij}(|\mathbf{p}|^2)$ used to construct optimized ground-state interpolating operators:

$$\chi_0(\mathbf{p}, t) = \sum_i w_{0i}(|\mathbf{p}|^2)\chi_i(\mathbf{p}, t). \tag{5}$$

These are used to construct two-point correlation functions as

$$C^{2\mathrm{pt}}_{0^{++}}(\mathbf{p}, t) = \frac{1}{T}\sum_{t_0}\langle\chi_0(\mathbf{p}, t + t_0)\chi_0(\mathbf{p}, t_0)^\dagger\rangle$$
$$= \sum_{i,j} w_{0i}(|\mathbf{p}|^2)C^{2\mathrm{pt}}_{ij}(\mathbf{p}, t)w^*_{0j}(|\mathbf{p}|^2). \tag{6}$$

For each $|\mathbf{p}|^2$, the generalized eigenvalue problem is then solved to extract the ground state, which is identified as the scalar glueball. Figures showing examples of the two-point correlation functions, and the corresponding analysis, are included in [53].

The matrix elements defined in Eq. (1) are obtained by using GEVP-optimized interpolating operators χ_0 to compute vacuum-subtracted three-point functions [49]

$$C^{3\mathrm{pt}}_{0^{++},\mathcal{R}\ell}(\mathbf{p}', \boldsymbol{\Delta}, t_s, \tau)$$
$$= \frac{1}{T}\sum_{t_0}\langle\chi_0(\mathbf{p}', t_s + t_0)T_{\mathcal{R}\ell}(\boldsymbol{\Delta}, \tau + t_0)\chi_0(\mathbf{p}', t_0)^\dagger\rangle \tag{7}$$

for $|\boldsymbol{\Delta}|^2 \leq 10(2\pi/L)^2$ and $|\mathbf{p}'|^2 \leq 6(2\pi/L)^2$. $T_{\mathcal{R}\ell}$ denotes the vacuum-subtracted gluon EMT projected to the ℓ row of the hypercubic group irreps [59] $\mathcal{R} \in \{\tau_1^{(3)}, \tau_3^{(6)}\}$. The individual EMT components are computed using the clover definition of the gluon field strength tensor, constructed using gluon links that have been acted on with two or three steps of stout smearing [44]. The two- and three-point correlation functions are then combined into ratios:

$$R_{0^{++},\mathcal{R}\ell}(\mathbf{p}', \boldsymbol{\Delta}, t_s, \tau)$$
$$= \frac{C^{3\mathrm{pt}}_{0^{++},\mathcal{R}\ell}(\mathbf{p}', \boldsymbol{\Delta}, t_s, \tau)}{C^{2\mathrm{pt}}_{0^{++}}(\mathbf{p}', t_s)}$$
$$\times\sqrt{\frac{C^{2\mathrm{pt}}_{0^{++}}(\mathbf{p}, t_s - \tau)}{C^{2\mathrm{pt}}_{0^{++}}(\mathbf{p}', t_s - \tau)}\frac{C^{2\mathrm{pt}}_{0^{++}}(\mathbf{p}', t_s)}{C^{2\mathrm{pt}}_{0^{++}}(\mathbf{p}, t_s)}\frac{C^{2\mathrm{pt}}_{0^{++}}(\mathbf{p}', \tau)}{C^{2\mathrm{pt}}_{0^{++}}(\mathbf{p}, \tau)}}$$
$$\xrightarrow[\tau, t_s-\tau\gg 0]{} \frac{\langle G[0^{++}](p')|T^{\mu\nu}|G[0^{++}](p)\rangle}{2\sqrt{E_{\mathbf{p}}E_{\mathbf{p}'}}}. \tag{8}$$

Ratios with choices of momenta, $\mathcal{R}$, and ℓ that result in the same linear combination of GFFs as defined in Eq. (1) are

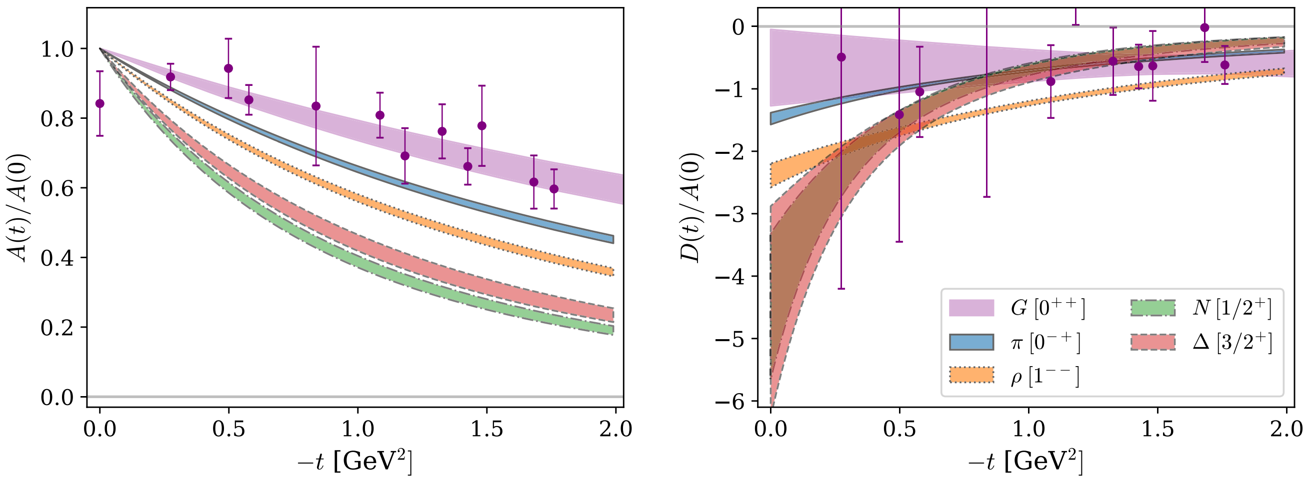

FIG. 1. Comparison of the t dependence of the $G[0^{++}]$ glueball GFFs in Yang-Mills theory obtained in this Letter, and the gluon GFFs of four other hadrons—the pion, ρ meson, nucleon, and Δ baryon, indicated with their J^P quantum numbers—obtained in a $N_f = 2 + 1$ lattice QCD calculation with $m_\pi \simeq 450$ MeV [72].

averaged. These averaged ratios are fit to extract the ground-state contribution. The fitting procedure is cross checked against recent generalizations of the Lanczos method [60–63], which provides statistically compatible results. Additional details, which closely follow previous lattice QCD studies of GFFs, e.g., Refs. [64–69], and figures showing the results of each analysis step, are given in [53].

Finally, the GFFs $A(t)$ and $D(t)$ are obtained by first grouping the fit results for the averaged ratios $\bar{R}_{0^{++},\mathcal{R}\ell}$ for each irrep $\mathcal{R}$ separately into 14 bins using k means clustering [70] on the momentum transfer squared $t = \Delta^2$, then solving the overconstrained systems of linear equations dictated by Eq. (1) to obtain the bare GFFs $A_\mathcal{R}(t)$ and $D_\mathcal{R}(t)$ for each irrep and bin. They can be renormalized by imposing the sum rule $A(0) = 1$. The renormalization factors $1/A^{\text{bare}}_\mathcal{R}(0)$ are obtained from a fit of an n-pole model $\alpha/(1 - t/\Lambda^2)^n$ to the bare GFF $A_\mathcal{R}(t)$; α and Λ are fitted parameters, and $\alpha = A^{\text{bare}}_\mathcal{R}(0)$. The bare GFFs in each momentum bin for each irrep are then multiplied by the renormalization factors, and then averaged together. Subsequently, the final results are obtained from a fit to the n-pole form, with α set to 1 to enforce $A(0) = 1$. Various analysis choices do not affect the results, as shown in [53]. Specifically, the choices $n \in \{1, 2, 3\}$ yield consistent values for the GFFs; in the main text $n = 3$. Similarly, separate analyses using the bare three-point functions with two and three steps of stout smearing are consistent; in the main text two steps of stout smearing are used, as the n pole fits to this data have a significantly larger p value.

Results—Figure 1 shows $A(t)$ and $D(t)$ of the 0^{++} glueball determined in this Letter. Also shown for comparison are the gluon GFFs, up to a factor [71] of $A(0)$, of four hadrons with quantum numbers $J^P = 0^-$, 1^-, $1/2^+$, and $3/2^+$, corresponding to the pion, ρ meson, nucleon, and Δ baryon, computed using a single lattice QCD ensemble with $N_f = 2 + 1$ clover-improved dynamical quark flavors, $a \simeq 0.12$ fm, and $m_\pi \simeq 450$ MeV [72]. While the present calculation is undertaken in Yang-Mills theory, this qualitative comparison may nevertheless yield interesting conclusions; a quenched calculation of the gluon GFFs of a pseudoscalar meson state with valence quark masses tuned such that the hadron mass matches that of Ref. [72] (shown in [53]) is consistent with the QCD results for the pion shown in Fig. 1, indicating that quenching has a negligible effect on these quantities at the level of uncertainties of this calculation. The glueball $A(t)$ form factor decays more slowly than that of the pion, corresponding to a smaller mass radius contribution. The same is observed in the respective D form factor, although the statistical uncertainty of $D(t)$ is larger for the glueball [73]. Naturally the situation in QCD will be somewhat more complicated; as noted previously, the scalar glueball in QCD is expected to mix substantially with other hadronic states [74–83].

Figure 2 shows a comparison of the results of this Letter with the *total* GFFs of the pion [65] and the nucleon [64], computed using an ensemble with the same action as in Ref. [72] but smaller lattice spacing $a \simeq 0.091$ fm and closer to the physical point with $m_\pi \simeq 170$ MeV. Since this comparison shows *total* GFFs, no division by $A(0)$ is necessary. The same qualitative conclusions are drawn; the glueball GFFs decay more slowly than those of the other hadrons, implying a smaller radius.

To carefully assess the radii comparison, we consider the root mean square radius of the energy density of the glueball in the Breit frame, also known as the mass radius. It is [30,84]

$$r^2_{\text{mass,BF}} = \frac{1}{A(0)}\left[6\frac{dA(t)}{dt}\bigg|_{t=0} - \frac{3}{4m^2}(A(0) + 2D(0))\right], \qquad (9)$$

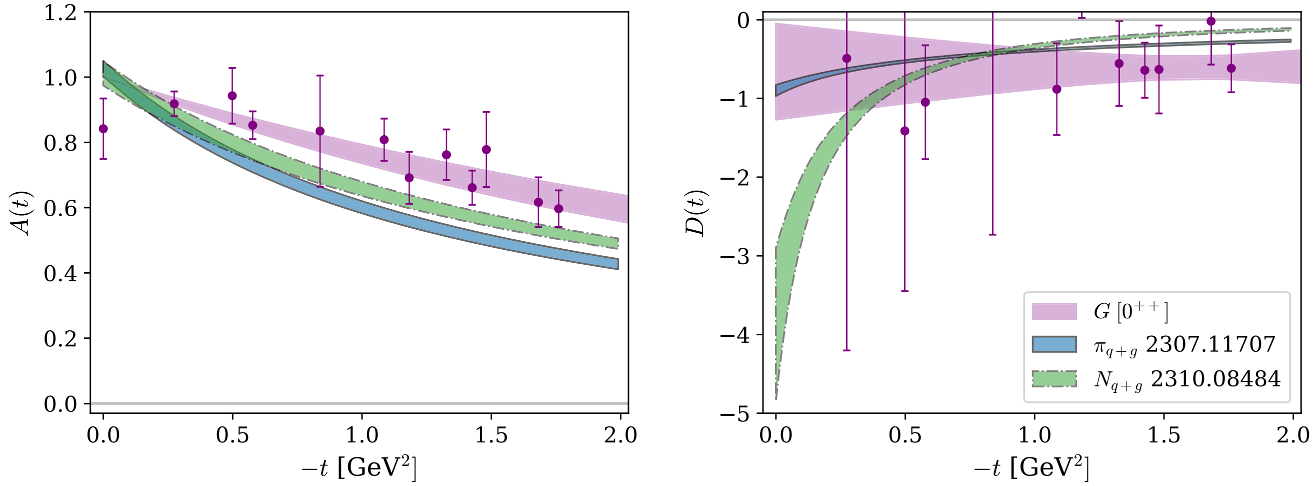

FIG. 2. Comparison between the $G[0^{++}]$ glueball GFFs in Yang-Mills theory obtained in this Letter, the total GFFs of the nucleon (using dipole fits) and the pion (using monopole fits) obtained with an $N_f = 2 + 1$ QCD ensemble with $m_\pi = 170$ MeV [64,65].

and is found to be 0.263(31) fm. This is remarkably small, and close to older lattice QCD and Bethe-Salpeter amplitude findings, which estimated the size of the scalar glueball to be in the range $0.1 - 0.3$ fm [19,20,22–24] by analyzing its (Bethe-Salpeter) wave function. This supports the view that the scalar glueball size is set by short-range gluon interactions (e.g., instanton-induced forces [19,20]) and not the confinement scale of QCD. It is also smaller than a dispersive prediction of the scalar radius of the σ meson [27], suggesting that the scalar glueball is the most compact state in that channel, though the absence of the σ in Yang-Mills could itself be contributing to the smallness [85].

Figure 3 shows a comparison of this quantity with the results of the n-pole fits of Refs. [64,72] for the other hadron states [86,87]. Note that other than for the pion, the BF mass radius of the rest of the hadrons depends on additional GFFs besides $A(t)$ and $D(t)$ [30,95–97], and their contribution is included in the radii values of Fig. 3 [98]. The scalar glueball radius is considerably smaller than that of the other hadrons.

Conclusion—These results constitute the first investigation of the internal structure of glueballs in an SU(3) lattice gauge theory, marking a promising advance in the understanding of the internal structure of potential glueball-like hadrons in nature.

While the calculation is undertaken in Yang-Mills theory instead of QCD, comparison with (quenched and full) QCD calculations of the (gluon and total) GFFs of other hadrons provides the first indication that glueballs may have a different gluonic structure than more typical hadronic states; specifically, the $A(t)$ GFF decays more slowly, corresponding to a smaller gluonic radius. This observation, if it is maintained in future QCD calculations of glueball GFFs, in particular once mixing between glueball and hadronic states is accounted for in that setting, might open the potential for future identification of glueball states directly via their gluon structure.

It would also be interesting to repeat this study with other glueball states in Yang-Mills theory, for instance with pseudoscalar or tensor quantum numbers. Notably, early lattice QCD studies based on wave function analyses suggested that the tensor glueball has a significantly larger radius than the scalar [22–24]. Future calculations could benefit from recent multi-level algorithm development [99,100].

The Chroma [101] and LALIBE [102] and JAX [103] libraries were used in this Letter. Data analysis used NumPy [104], SciPy [105], LSQFIT [106], and GVAR [107]. Figures were produced using Matplotlib [108].

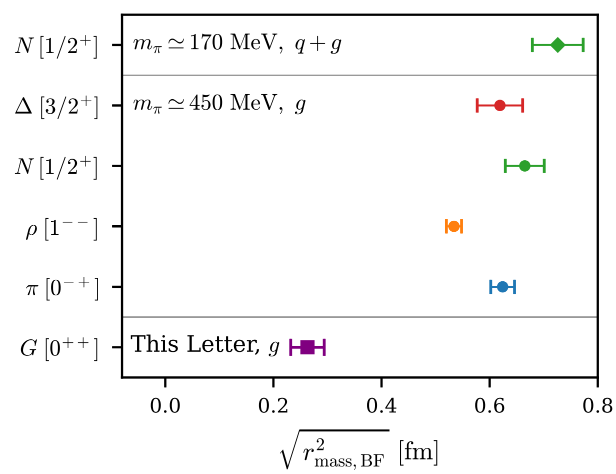

FIG. 3. The total (purely gluonic) mass radius of the glueball in the Breit frame obtained in this Letter, in units of fm, compared with the gluon contribution to the BF mass radius of the pion, ρ meson, nucleon, and Δ baryon extracted in a lattice QCD calculation with a heavier than physical pion mass $m_\pi \simeq 450$ MeV, as well as the *total* mass radius of the nucleon extracted at $m_\pi \simeq 170$ MeV [64,65].

Acknowledgments—The authors thank Julian Urban for contributions at early stages of the project. We also thank Lorenzo Barca, Max Hansen, Gerrit Schierholz, André Walker-Loud, and Roman Zwicky for useful discussions. P. E. S. is supported in part by the U.S. Department of Energy, Office of Science, Office of Nuclear Physics, under Grant Contract No. DE-SC0011090, by Early Career Award No. DE-SC0021006, by Simons Foundation Grant No. 994314 (Simons Collaboration on Confinement and QCD Strings), by the U.S. Department of Energy SciDAC5 Award No. DE-SC0023116, and has benefited from the QGT Topical Collaboration No. DE-SC0023646. D. A. P. is supported from the Office of Nuclear Physics, Department of Energy, under Contract No. DE-SC0004658. This document was prepared using the resources of the Fermi National Accelerator Laboratory (Fermilab), a US Department of Energy, Office of Science, Office of High Energy Physics HEP User Facility. Fermilab is managed by Fermi Forward Discovery Group, LLC, acting under Contract No. 89243024CSC000002. R. A. is supported by the US Department of Energy SciDAC5 Award No. DE-SC0023116 and the High Energy Physics Computing Traineeship for Lattice Gauge Theory (No. DE-SC0024053). This research used resources of the National Energy Research Scientific Computing Center (NERSC), a US Department of Energy Office of Science User Facility operated under Contract No. DE-AC02-05CH11231. The authors acknowledge the MIT SuperCloud [109] and Lincoln Laboratory Supercomputing Center for providing HPC resources that have contributed to the research results reported within this Letter. This work made use of resources provided by subMIT at MIT Physics [110]. P. E. S. thanks the Institute for Nuclear Theory at the University of Washington for its kind hospitality and stimulating research environment. D. A. P. thanks the Albert Einstein Center at the University of Bern for its hospitality during a visit that significantly advanced this work. This research was supported in part by the INT's US Department of Energy Grant No. DE-FG02-00ER41132. This manuscript was finalized at Aspen Center for Physics, which is supported by National Science Foundation Grant No. PHY-2210452.

Data availability—The data for the figures of this article are openly available [111]. All raw data corresponding to the findings of the manuscript are not publicly available upon publication because it is not technically feasible and/or the cost of preparing, depositing, and hosting the data would be prohibitive within the terms of this research project. The data are available from the authors upon reasonable request.

[1] H. Fritzsch and M. Gell-Mann, Current algebra: Quarks and what else?, eConf **C720906V2**, 135 (1972).

[2] E. Klempt and A. Zaitsev, Glueballs, hybrids, multiquarks. Experimental facts versus QCD inspired concepts, Phys. Rep. **454**, 1 (2007).

[3] V. Crede and C. A. Meyer, The experimental status of glueballs, Prog. Part. Nucl. Phys. **63**, 74 (2009).

[4] H.-X. Chen, W. Chen, X. Liu, Y.-R. Liu, and S.-L. Zhu, An updated review of the new hadron states, Rep. Prog. Phys. **86**, 026201 (2023).

[5] M. Ablikim *et al.* (BESIII Collaboration), Confirmation of the $X(1835)$ and observation of the resonances $X(2120)$ and $X(2370)$ in $J/\psi \to \gamma\pi^+\pi^-\eta'$, Phys. Rev. Lett. **106**, 072002 (2011).

[6] M. Ablikim *et al.* (BESIII Collaboration), Observation of $X(2370)$ and search for X(2120) in $J/\psi \to \gamma K\bar{K}\eta'$, Eur. Phys. J. C **80**, 746 (2020).

[7] M. Ablikim *et al.* (BESIII Collaboration), Determination of spin-parity quantum numbers of X(2370) as 0^{-+} from $J/\psi \to \gamma K^0_S K^0_S \eta'$', Phys. Rev. Lett. **132**, 181901 (2024).

[8] M. J. Teper, Glueball masses and other physical properties of SU(N) gauge theories in $D = (3+1)$: A review of lattice results for theorists, arXiv:hep-th/9812187.

[9] C. J. Morningstar and M. J. Peardon, The Glueball spectrum from an anisotropic lattice study, Phys. Rev. D **60**, 034509 (1999).

[10] A. Athenodorou and M. Teper, SU(N) gauge theories in $2+1$ dimensions: Glueball spectra and k-string tensions, J. High Energy Phys. 02 (2017) 015.

[11] A. Athenodorou and M. Teper, The glueball spectrum of SU(3) gauge theory in $3+1$ dimensions, J. High Energy Phys. 11 (2020) 172.

[12] K. Sakai and S. Sasaki, Glueball spectroscopy in lattice QCD using gradient flow, Phys. Rev. D **107**, 034510 (2023).

[13] G. S. Bali, B. Bolder, N. Eicker, T. Lippert, B. Orth, P. Ueberholz, K. Schilling, and T. Struckmann (TXL Collaboration and T(X)L Collaboration), Static potentials and glueball masses from QCD simulations with Wilson sea quarks, Phys. Rev. D **62**, 054503 (2000).

[14] A. Athenodorou, J. Finkenrath, A. Lantos, and M. Teper, Glueball spectrum with four light dynamical fermions, arXiv:2308.10054.

[15] D. Vadacchino, A review on Glueball hunting, in *Proceedings of the 39th International Symposium on Lattice Field Theory* (2023).

[16] C. Morningstar, Update on glueballs, Proc. Sci. LATTICE2024 (**2024**) 004 [arXiv:2502.02547].

[17] C. Amsler and F. E. Close, Evidence for a scalar glueball, Phys. Lett. B **353**, 385 (1995).

[18] C. Amsler and F. E. Close, Is $f_0(1500)$ a scalar glueball?, Phys. Rev. D **53**, 295 (1996).

[19] T. Schäfer and E. V. Shuryak, Glueballs and instantons, Phys. Rev. Lett. **75**, 1707 (1995).

[20] H. Forkel, Scalar gluonium and instantons, Phys. Rev. D **64**, 034015 (2001).

[21] W.-S. Hou and G.-G. Wong, The Glueball spectrum from a potential model, Phys. Rev. D **67**, 034003 (2003).

[22] R. Gupta, A. Patel, C. F. Baillie, G. W. Kilcup, and S. R. Sharpe, Exploring glueball wave functions on the lattice, Phys. Rev. D **43**, 2301 (1991).

[23] P. de Forcrand and K.-F. Liu, Glueball wave functions in lattice gauge calculations, Phys. Rev. Lett. **69**, 245 (1992).

[24] M. Loan and Y. Ying, Sizes of lightest glueballs in SU(3) lattice gauge theory, Prog. Theor. Phys. **116**, 169 (2006).

[25] G. A. Tickle and C. Michael, An investigation of the structure of the 0^+ glueball in SU(2) lattice gauge theory, Nucl. Phys. **B333**, 593 (1990).

[26] K. Ishikawa, G. Schierholz, H. Schneider, and M. Teper, On investigating the structure of hadrons: Lattice Monte Carlo measurements of color magnetic and electric fields and the topological charge density inside glueballs, Nucl. Phys. **B227**, 221 (1983).

[27] M. Albaladejo and J. A. Oller, On the size of the sigma meson and its nature, Phys. Rev. D **86**, 034003 (2012).

[28] M. Polyakov, Generalized parton distributions and strong forces inside nucleons and nuclei, Phys. Lett. B **555**, 57 (2003).

[29] C. Lorcé, H. Moutarde, and A. P. Trawiński, Revisiting the mechanical properties of the nucleon, Eur. Phys. J. C **79**, 89 (2019).

[30] M. V. Polyakov and P. Schweitzer, Forces inside hadrons: Pressure, surface tension, mechanical radius, and all that, Int. J. Mod. Phys. A **33**, 1830025 (2018).

[31] V. D. Burkert, L. Elouadrhiri, F. X. Girod, C. Lorcé, P. Schweitzer, and P. E. Shanahan, Colloquium: Gravitational form factors of the proton, Rev. Mod. Phys. **95**, 041002 (2023).

[32] Y. Chen *et al.*, Glueball spectrum and matrix elements on anisotropic lattices, Phys. Rev. D **73**, 014516 (2006).

[33] R. Abbott, D. C. Hackett, D. A. Pefkou, F. Romero-López, and P. Shanahan, Gravitational form factors of glueballs in Yang-Mills theory, Proc. Sci. LATTICE2024 (**2025**) 459 [arXiv:2410.02706].

[34] H. Pagels, Energy-momentum structure form factors of particles, Phys. Rev. **144**, 1250 (1966).

[35] J. Hudson and P. Schweitzer, D term and the structure of pointlike and composed spin-0 particles, Phys. Rev. D **96**, 114013 (2017).

[36] S. Cotogno, C. Lorcé, P. Lowdon, and M. Morales, Covariant multipole expansion of local currents for massive states of any spin, Phys. Rev. D **101**, 056016 (2020).

[37] S. Necco and R. Sommer, The $N_f = 0$ heavy quark potential from short to intermediate distances, Nucl. Phys. **B622**, 328 (2002).

[38] S. Durr, Z. Fodor, C. Hoelbling, and T. Kurth, Precision study of the SU(3) topological susceptibility in the continuum, J. High Energy Phys. 04 (2007) 055.

[39] M. Creutz, Monte Carlo study of quantized SU(2) gauge theory, Phys. Rev. D **21**, 2308 (1980).

[40] N. Cabibbo and E. Marinari, A new method for updating SU(N) matrices in computer simulations of gauge theories, Phys. Lett. **119B**, 387 (1982).

[41] A. D. Kennedy and B. J. Pendleton, Improved heat bath method for Monte Carlo calculations in lattice gauge theories, Phys. Lett. **156B**, 393 (1985).

[42] F. R. Brown and T. J. Woch, Overrelaxed Heat bath and metropolis algorithms for accelerating pure gauge Monte Carlo calculations, Phys. Rev. Lett. **58**, 2394 (1987).

[43] S. L. Adler, Overrelaxation algorithms for lattice field theories, Phys. Rev. D **37**, 458 (1988).

[44] C. Morningstar and M. J. Peardon, Analytic smearing of SU(3) link variables in lattice QCD, Phys. Rev. D **69**, 054501 (2004).

[45] C. Michael, Torelons and unusual ground states, Phys. Lett. B **232**, 247 (1989).

[46] G. Fox, R. Gupta, O. Martin, and S. Otto, Monte Carlo estimates of the mass gap of the O(2) and O(3) spin models in $(1+1)$-dimensions, Nucl. Phys. **B205**, 188 (1982).

[47] C. Michael and I. Teasdale, Extracting glueball masses from Lattice QCD, Nucl. Phys. **B215**, 433 (1983).

[48] M. Luscher and U. Wolff, How to calculate the elastic scattering matrix in two-dimensional quantum field theories by numerical simulation, Nucl. Phys. **B339**, 222 (1990).

[49] B. Blossier, M. Della Morte, G. von Hippel, T. Mendes, and R. Sommer, On the generalized eigenvalue method for energies and matrix elements in lattice field theory, J. High Energy Phys. 04 (2009) 094.

[50] G. T. Fleming, Beyond generalized eigenvalues in lattice quantum field theory, in *Proceedings of the 40th International Symposium on Lattice Field Theory* (2023).

[51] M. Fischer, B. Kostrzewa, J. Ostmeyer, K. Ottnad, M. Ueding, and C. Urbach, On the generalised eigenvalue method and its relation to Prony and generalised pencil of function methods, Eur. Phys. J. A **56**, 206 (2020).

[52] G. F. Sterman and W. Vogelsang, Soft gluon resummation and PDF theory uncertainties, in *Physics at Run II: QCD and Weak Boson Physics Workshop: Final General Meeting* (2000).

[53] See Supplemental Material at http://link.aps.org/supplemental/10.1103/67xg-qxhz, which also includes Refs. [54–58], for additional analysis details and discussion.

[54] W. I. Jay and E. T. Neil, Bayesian model averaging for analysis of lattice field theory results, Phys. Rev. D **103**, 114502 (2021).

[55] E. Rinaldi, S. Syritsyn, M. L. Wagman, M. I. Buchoff, C. Schroeder, and J. Wasem, Neutron-antineutron oscillations from lattice QCD, Phys. Rev. Lett. **122**, 162001 (2019).

[56] S. R. Beane, E. Chang, W. Detmold, K. Orginos, A. Parreño, M. J. Savage, and B. C. Tiburzi (NPLQCD Collaboration), Ab initio calculation of the $np \to d\gamma$ radiative capture process, Phys. Rev. Lett. **115**, 132001 (2015).

[57] M. Luscher and P. Weisz, On-shell improved lattice gauge theories, Commun. Math. Phys. **98**, 433 (1985); **98**, 433(E) (1985).

[58] B. Sheikholeslami and R. Wohlert, Improved continuum limit lattice action for QCD with Wilson fermions, Nucl. Phys. **B259**, 572 (1985).

[59] M. Gockeler, R. Horsley, E.-M. Ilgenfritz, H. Perlt, P. E. L. Rakow, G. Schierholz, and A. Schiller, Lattice operators for moments of the structure functions and their transformation under the hypercubic group, Phys. Rev. D **54**, 5705 (1996).

[60] M. L. Wagman, Lanczos algorithm, the transfer matrix, and the signal-to-noise problem, Phys. Rev. Lett. **134**, 241901 (2025).

[61] D. C. Hackett and M. L. Wagman, Lanczos for Lattice QCD matrix elements, Phys. Rev. D **112**, 054506 (2025).

[62] D. C. Hackett and M. L. Wagman, Block Lanczos algorithm for lattice QCD spectroscopy and matrix elements, Phys. Rev. D **112**, 014514 (2025).

[63] R. Abbott, D. C. Hackett, G. T. Fleming, D. A. Pefkou, and M. L. Wagman, Filtered Rayleigh-Ritz is all you need, arXiv:2503.17357.

[64] D. C. Hackett, D. A. Pefkou, and P. E. Shanahan, Gravitational form factors of the proton from Lattice QCD, Phys. Rev. Lett. **132**, 251904 (2024).

[65] D. C. Hackett, P. R. Oare, D. A. Pefkou, and P. E. Shanahan, Gravitational form factors of the pion from Lattice QCD, Phys. Rev. D **108**, 114504 (2023).

[66] D. Brömmel, Pion structure from the Lattice, Ph.D. thesis, Regensburg University, 2007.

[67] W. Detmold, D. Pefkou, and P. E. Shanahan, Off-forward gluonic structure of vector mesons, Phys. Rev. D **95**, 114515 (2017).

[68] P. Shanahan and W. Detmold, Gluon gravitational form factors of the nucleon and the pion from Lattice QCD, Phys. Rev. D **99**, 014511 (2019).

[69] P. Shanahan and W. Detmold, Pressure distribution and shear forces inside the proton, Phys. Rev. Lett. **122**, 072003 (2019).

[70] D. Steinberg, kmeans1d, https://github.com/dstein64/kmeans1d (2019).

[71] Mesons and baryons with valence quarks and antiquarks also receive a quark contribution to their GFFs, which mixes with the gluonic component. The work of Ref. [72] constrained only the gluon contribution of the GFFs, also neglecting the mixing. The comparison of the overall normalization between those results and the gluon GFFs in this work—which coincide with the total GFFs in a theory with only gluonic degrees of freedom, as investigated here—is not meaningful.

[72] D. A. Pefkou, D. C. Hackett, and P. E. Shanahan, Gluon gravitational structure of hadrons of different spin, Phys. Rev. D **105**, 054509 (2022).

[73] The flat t dependence of $D(t)$ is difficult to interpret at this level of statistics, especially when taking into consideration the three-stout smeared result shown in [53], where the behavior is more consistent with monotonically increasing.

[74] L. Burakovsky and P. R. Page, Scalar glueball mixing and decay, Phys. Rev. D **59**, 014022 (1999); **59**, 079902(E) (1999).

[75] C. McNeile and C. Michael (UKQCD Collaboration), Mixing of scalar glueballs and flavor singlet scalar mesons, Phys. Rev. D **63**, 114503 (2001).

[76] F. Giacosa, T. Gutsche, V. E. Lyubovitskij, and A. Faessler, Scalar nonet quarkonia and the scalar glueball: Mixing and decays in an effective chiral approach, Phys. Rev. D **72**, 094006 (2005).

[77] H.-Y. Cheng, C.-K. Chua, and K.-F. Liu, Scalar glueball, scalar quarkonia, and their mixing, Phys. Rev. D **74**, 094005 (2006).

[78] H. Noshad, S. Mohammad Zebarjad, and S. Zarepour, Mixing among lowest-lying scalar mesons and scalar glueball, Nucl. Phys. **B934**, 408 (2018).

[79] X.-D. Guo, H.-W. Ke, M.-G. Zhao, L. Tang, and X.-Q. Li, Revisiting the determining fraction of glueball component in f_0 mesons via radiative decays of J/ψ, Chin. Phys. C **45**, 023104 (2021).

[80] F. J. Llanes-Estrada, Glueballs as the Ithaca of meson spectroscopy: From simple theory to challenging detection, Eur. Phys. J. Special Topics **230**, 1575 (2021).

[81] J.-L. Ren, M.-Q. Li, X. Liu, Z.-T. Zou, Y. Li, and Z.-J. Xiao, The $B^0 \to J/\psi f_0(1370, 1500, 1710)$ decays: An opportunity for scalar glueball hunting, Eur. Phys. J. C **84**, 358 (2024).

[82] A. V. Sarantsev, I. Denisenko, U. Thoma, and E. Klempt, Scalar isoscalar mesons and the scalar glueball from radiative J/ψ decays, Phys. Lett. B **816**, 136227 (2021).

[83] E. Klempt and A. V. Sarantsev, Singlet-octet-glueball mixing of scalar mesons, Phys. Lett. B **826**, 136906 (2022).

[84] A. Freese and I. C. Cloët, Gravitational form factors of light mesons, Phys. Rev. C **100**, 015201 (2019); **105**, 059901(E) (2022).

[85] R. Stegeman and R. Zwicky, Gravitational D-form factor: The σ-meson as a dilaton confronted with lattice data, arXiv:2508.18537.

[86] The numbers in Fig. 3 taken from Ref. [72] differ from those currently in Table X of the published article. This is due to an error in normalization in the results of that table only; an erratum is forthcoming.

[87] We do not compare with the radius of the $m_\pi \simeq 170$ MeV pion study of Ref. [65], because for light hadrons the 3D BF density interpretation is expected to break down [29,88–94].

[88] D. R. Yennie, M. M. Lévy, and D. G. Ravenhall, Electromagnetic structure of nucleons, Rev. Mod. Phys. **29**, 144 (1957).

[89] M. Burkardt, Impact parameter space interpretation for generalized parton distributions, Int. J. Mod. Phys. A **18**, 173 (2003).

[90] G. A. Miller, Defining the proton radius: A unified treatment, Phys. Rev. C **99**, 035202 (2019).

[91] R. L. Jaffe, Ambiguities in the definition of local spatial densities in light hadrons, Phys. Rev. D **103**, 016017 (2021).

[92] E. Epelbaum, J. Gegelia, N. Lange, U. G. Meißner, and M. V. Polyakov, Definition of local spatial densities in hadrons, Phys. Rev. Lett. **129**, 012001 (2022).

[93] A. Freese and G. A. Miller, Forces within hadrons on the light front, Phys. Rev. D **103**, 094023 (2021).

[94] A. Freese, Mechanical form factors and densities of nonrelativistic fermions, Phys. Rev. D **112**, 034037 (2025).

[95] M. V. Polyakov and B.-D. Sun, Gravitational form factors of a spin one particle, Phys. Rev. D **100**, 036003 (2019).

[96] B.-D. Sun and Y.-B. Dong, Gravitational form factors of ρ meson with a light-cone constituent quark model, Phys. Rev. D **101**, 096008 (2020).

[97] J.-Y. Kim and B.-D. Sun, Gravitational form factors of a baryon with spin-3/2, Eur. Phys. J. C **81**, 85 (2021).

[98] We do not compare with the radius of the $m_\pi \simeq 170$ MeV pion study of Ref. [65], because for light hadrons the 3D BF density interpretation is expected to break down [29,88–94].

[99] L. Barca, S. Schaefer, F. Knechtli, J. A. Urrea-Niño, S. Martins, and M. Peardon, Exponential error reduction for glueball calculations using a two-level algorithm in pure gauge theory, Phys. Rev. D **110**, 054515 (2024).

[100] L. Barca, J. Finkenrath, F. Knechtli, M. J. Peardon, S. Schaefer, and J. A. Urrea-Niño, Update on two-level sampling for glueball observables in quenched QCD, Proc. Sci. LATTICE2024 (**2025**) 062 [arXiv:2501.17988].

[101] R. G. Edwards and B. Joó (SciDAC Collaboration, LHPC Collaboration, and UKQCD Collaboration), The Chroma software system for lattice QCD, Nucl. Phys. B, Proc. Suppl. **140**, 832 (2005).

[102] A. Gambhir, D. Brantley, J. Chang, B. Hörz, H. Monge-Camacho, P. Vranas, and A. Walker-Loud, LALIBE, https://github.com/callat-qcd/lalibe (2018).

[103] J. Bradbury, R. Frostig, P. Hawkins, M. J. Johnson, C. Leary, D. Maclaurin, G. Necula, A. Paszke, J. VanderPlas, S. Wanderman-Milne, and Q. Zhang, JAX: Composable transformations of Python + NumPy programs, (2018), http://github.com/jax-ml/jax.

[104] C. R. Harris *et al.*, Array programming with NumPy, Nature (London) **585**, 357 (2020).

[105] P. Virtanen *et al.* (SciPySciPy 1.0 Contributors), SciPy 1.0: Fundamental algorithms for scientific computing in Python, Nat. Methods **17**, 261 (2020).

[106] G. P. Lepage, LSQFIT v. 11.7, 10.5281/zenodo.4037174 (2020), https://github.com/gplepage/lsqfit.

[107] G. P. Lepage, GVAR v. 11.9.1, 10.5281/zenodo.4290884 (2020), https://github.com/gplepage/gvar.

[108] J. D. Hunter, Matplotlib: A 2d graphics environment, Comput. Sci. Eng. **9**, 90 (2007).

[109] A. Reuther, J. Kepner, C. Byun, S. Samsi, W. Arcand, D. Bestor, B. Bergeron, V. Gadepally, M. Houle, M. Hubbell, M. Jones, A. Klein, L. Milechin, J. Mullen, A. Prout, A. Rosa, C. Yee, and P. Michaleas, Interactive supercomputing on 40,000 cores for machine learning and data analysis, in *2018 IEEE High Performance extreme Computing Conference (HPEC)* (IEEE, New York, 2018), pp. 1–6.

[110] J. Bendavid, M. D'Alfonso, J. Eysermans, C. Freer, M. Goncharov, M. Heine, L. Lavezzo, M. Moore, C. Paus, X. Shen, D. Walter, and Z. Wang, SubMIT: A physics analysis facility at MIT, arXiv:2506.01958.

[111] 10.5281/zenodo.17103070.